



Published in final edited form as:

*Radiat Res.* 2009 December ; 172(6): 653–665. doi:10.1667/RR1926.1.

## Relationships between Cycling Hypoxia, HIF-1, Angiogenesis and Oxidative Stress

Mark W. Dewhirst<sup>1</sup>

Radiation Oncology Department, Duke University Medical Center, Durham, North Carolina 27710

### Abstract

This Failla Lecture focused on the inter-relationships between tumor angiogenesis, HIF-1 expression and radiotherapy responses. A common thread that bonds all of these factors together is microenvironmental stress caused by reactive oxygen and nitrogen species formed during tumor growth and angiogenesis or in response to cytotoxic treatment. In this review we focus on one aspect of the crossroad between oxidative stress and angiogenesis, namely cycling hypoxia. Understanding of the relative importance of this feature of the tumor microenvironment has recently expanded; it influences tumor biology in ways that are separate from chronic hypoxia. Cycling hypoxia can influence angiogenesis, treatment responses and metastatic behavior. It represents an important and relatively less well understood feature of tumor biology that requires additional research.

### INTRODUCTION

Tumor hypoxia has been one of the most intensively studied features of the tumor microenvironment. Historically, the relative resistance of hypoxic tumor cells to radiation treatment has led to numerous radiobiological studies of tumor hypoxia, but in more recent years, the recognition that hypoxia causes alterations in cellular function has led to a literal explosion of publications in this field. The ISI Science Citation Index™ lists over 7000 publications with key terms of “tumor” and “hypoxia”. Roughly 1100 of these also include the term “radiation”. The annual number of citations that use the term “hypoxia” reached exponential growth starting in the early 1990s. The dramatic increase in citations coincided with the discovery of hypoxia-inducible factor 1 (HIF-1), a heterodimeric transcription factor that promotes up-regulation of hypoxia-inducible genes (1,2). Among the most highly cited papers are several involving angiogenesis (3-5), because HIF-1 is known to up-regulate pro-angiogenic factors, such as vascular endothelial growth factor (VEGF). Thus it is imperative that one consider tumor hypoxia in the context of angiogenesis. These two aspects of tumor pathophysiology are inextricably connected.

We have recently summarized tumor hypoxia as having eight dominant features (6): (a) A relatively sparse arteriolar supply reduces the amount of oxygenated blood that enters the tumor. This leads to very low oxygen concentrations of tumor microvessels that are far removed from the arteriolar source (7-9). (b) Inefficient orientation of tumor blood vessels leads to an overabundance of vasculature in some regions and insufficient density in others. Such differences can be observed in very small tumor regions that are barely larger than the diffusion distance of oxygen (10) and (c) on a larger scale, such as comparing tumor periphery with tumor center; vascular density is typically lower in the second case. (d) Large variations in red

cell flux (the number of red blood cells that traverse a microvessel per unit time) are observed. Some tumor microvessels contain very few to no red blood cells (11). (e) Hypoxic red blood cells shrink and become stiffer than normally oxygenated cells (12). This increases blood viscosity, slowing flow and affecting distribution of red blood cells at vascular bifurcations. (f) Large-diameter shunts between arteriolar and draining veins divert blood away from the tumor mass (13). (g) The demand for oxygen can be higher than the supply (14).

Temporally unstable oxygen transport is the eighth feature of tumor hypoxia. This occurs as a result of instabilities in microvessel red blood cell flux (6). This complex feature of tumor hypoxia is the focus of this review. We will provide a historical overview describing how this was first discovered and will end with a modern perspective on its essential features and a discussion regarding its relative importance in influencing tumor biology and treatment responses. Temporal instability in oxygen transport has classically been termed “intermittent” or “acute” hypoxia. We and others recently suggested using the term “cycling”, because it more clearly indicates that this process is dynamic (6,15).

The kinetics of cycling hypoxia is complex, involving cycle times that range from a few cycles per hour to many hours or days. The spatial characteristics of cycling hypoxia most commonly involve networks of microvessels as opposed to isolated blood vessels. As such, it can involve large tumor regions, as opposed to occurring in isolation. Below, we will review the key literature on this subject and will provide a composite model of how all of this fits together.

## HISTORICAL PERSPECTIVE

Intravital microscopy, the observation of microvascular function in living animals, has been a valuable experimental tool for over 80 years. The first “window chamber” model was developed in the rabbit ear (16), followed by the hamster cheek pouch (17) and the dorsal skin fold window chamber (18). The ability to serially monitor blood flow using intravital microscopy of these models was a key to observing instability in microvessel perfusion. Goodall *et al.* were among the first to mention that regurgitant flow and transient stasis occurred in tumors growing in hamster cheek pouch (17). Eddy occasionally observed vascular stasis in coopted normal microvessels of a developing neurilemmoma using the hamster cheek pouch model, but neither he nor Goodall speculated on the significance of this observation (13). Endrich was one of the first to directly measure flow rates in tumor microvessels in melanomas growing in the hamster skin flap. Small tumors were reported to have very few microvessels exhibiting vascular stasis, but as they grew to sizes approximating the size of the window, the appearance of vascular stasis increased (19). We reported that the incidence of total vascular stasis in mammary tumors growing in window chambers of rats was less than 5%, and when it did happen, it typically lasted less than 1 min (11). The influence of vascular stasis on tissue oxygenation will be discussed below.

Two key papers were published in the late 1970s that put a radiobiological perspective on the potential importance of cycling hypoxia. Yamaura performed detailed analyses of hepatoma regrowth in window chambers after a single 30-Gy dose of radiation. The center of the tumors was completely destroyed; tumor regrowth occurred predominantly at the tumor periphery. They were convinced that the primary mechanism for this must have been due to a larger fraction of tumor cells being in the relatively radioresistant S phase of the cell cycle, but they also mentioned that this might have been due to transient hypoxia, because they occasionally observed temporary vascular stasis in the tumor periphery (20). Brown performed a classic study to demonstrate directly that cycling hypoxia could be a cause for radioresistance. He used the EMT6 mammary carcinoma, which can be studied radiobiologically as an *in vivo-in vitro* assay. Here the tumor is irradiated *in situ* and then disaggregated and plated out to determine surviving fraction *in vitro*, using a standard colonyforming assay (21). In intradermal

tumors, there was a clear biphasic survival curve, with the terminal slope being parallel to that of hypoxic tumor cells. This indicated that there was a hypoxic subfraction of cells in this site of tumor growth. When tumor-bearing mice were treated with misonidazole, a selective hypoxic cytotoxin, 24 h prior to irradiation, a radiobiologically resistant subpopulation of tumor cells was still evident. Brown concluded that some of the surviving aerobic tumor cells after misonidazole treatment must have become hypoxic before irradiation (22). Note that the Brown study evaluated a change in hypoxia over 24 h, whereas Yamaura studied flow dynamics over less than an hour.

Chaplin and Durand made significant strides in understanding cycling hypoxia by using a clever indirect method of marking tumor cells residing near blood vessels with a perfusion marker dye (23). This was done by administering the DNA-binding dye Hoechst 33342 intravenously, irradiating the tumor and then removing the tumors a few minutes later to assess surviving fraction using the clonogenic assay. The tumors were disaggregated into single cells and sorted by flow cytometry by the intensity of dye staining. Brightly stained cells were considered those that were near blood vessels and therefore were better oxygenated. When they administered the dye simultaneously with radiation, the most brightly stained cells were clearly more radiosensitive. However, if they waited 20 min between dye administration and irradiation, there was no difference in radiosensitivity between the brightly and dimly stained cells. This result suggested that the hypoxic fraction of cells was changing over the 20-min interval and that cells that were aerobic at the beginning of the 20-min interval were hypoxic at the end of that interval. This seminal observation indicated that there was periodicity in tumor oxygenation with a time scale of a few cycles per hour.

These two investigators went on to extend their methods to ask what fraction of tumor cells were experiencing cycling hypoxia. They used two fluorescent dyes (or fluorescent beads that were trapped in tumor microvessels) and administered them together or separated in time. Subsequently, they removed the tumors and looked for overlap in fluorescence between the two markers as a function of time between the two injections. In their initial studies with this method they looked for regions of complete mismatch and then later extended this to examine differences in fluorescence intensity (24,25). In the latter case, it was clear that large tumor regions were experiencing large fluctuations in perfusion. More recently, they used matched hypoxia marker drugs to examine this same type of question (26,27), concluding that changes in oxygenation state occur over prolonged periods of up to several hours (26,27). Hypoxia marker drugs are selectively retained in viable hypoxic cells and can be detected in tissues using immunohistochemistry (28,29). Bennewith *et al.* estimated that up to 20% of tumor cells could experience cycling hypoxia over periods of several hours, depending upon the tumor type and size of tumor. They also concluded that these cells were typically not immediately adjacent to tumor microvessels (26).

Collectively, these studies demonstrated that cycling hypoxia was a common feature of rodent tumors and that it has significant radiobiological implications. It was not clear whether vascular stasis was the culprit. More information was clearly needed. Listed below were some unanswered questions:

1. What is the underlying cause for cycling hypoxia?
2. What is the kinetics of cycling hypoxia?
3. What are the spatial characteristics, and are there methods to study cycling hypoxia using imaging techniques, particularly those that could be used clinically?
4. Are chronic and cycling hypoxia distinct pathophysiological entities within tumors, or do they emanate from the same underlying pathology?

5. Are the consequences of cycling hypoxia different from those associated with chronic hypoxia?
6. Does cycling hypoxia occur in human tumors? If so, is it clinically relevant?

We will now address each of these questions.

## WHAT IS THE UNDERLYING MECHANISM FOR CYCLING HYPOXIA?

The oxygenation of any tissue is dependent upon the balance between delivery and consumption. In the most general sense, cycling hypoxia must result from changes in delivery or changes in oxygen consumption rate. To date, there have not been any detailed analyses of variations in oxygen consumption rate over time, but there have been extensive studies on fluctuations of perfusion and red cell flux. Our discussion will focus on this latter topic.

Helmlinger *et al.* combined measurements of microvessel blood flow rate with an optical method for measuring tissue  $pO_2$  called phosphorescence lifetime imaging; these studies were performed in skin fold window chambers (30). Phosphorescence lifetime imaging involves administering a Pd-porphyrin dye that phosphoresces when illuminated with visible light. The lifetime of the phosphorescence is dependent on oxygen (31). They observed temporal fluctuations in  $pO_2$ , but these were not correlated with variations in perfusion rate. Recently we have reported correlations between perfusion rate, measured with optical coherence tomography (OCT) and hemoglobin saturation of the same blood vessels, as serially assessed over several hours (32). We believe that the difference between our result and the earlier one by Helmlinger may be due to the fact that with OCT we are able to account for the angle of the vessel, which cannot be done with a simple epiillumination system. This will give a more precise velocity measurement.

Kimura *et al.* used a combination of fluorescence microscopy to measure red cell flux in skin fold window chamber tumors while simultaneously measuring perivascular  $pO_2$  with oxygen microelectrodes (33). Clear correlations between red cell flux and  $pO_2$  were observed, but the slope of the correlation curve was dependent upon vascular density in the region of the measurement. Regions with high vascular density were less affected by fluctuations in red cell flux of one microvessel. More recently, we demonstrated that correlations exist between red cell flux of microvessels and interstitial  $pO_2$ , extending to the diffusion distance of oxygen (34). These results strongly suggest that a primary determinant of cycling hypoxia is variation in microvessel red blood cell flux (Fig. 1).

What we do not yet know is what causes variation in red cell flux and perfusion. In one series of experiments we were able to demonstrate a correlation between slow vasomotor activity of tumor feeding arterioles and downstream red cell flux (11), but this was inconsistent and is not likely to be the only cause for variations. Vascular remodeling may also be responsible for this. Changes in vascular network hemodynamics are highly influenced by even small changes in flow patterns (35). This might result from processes such as vascular pruning, connection of new vascular loops and intussusception (36,37). Additional studies to uncover the underlying mechanisms for cycling hypoxia may permit the discovery of ways to reduce its magnitude or frequency within tumors.

## WHAT IS THE KINETICS OF CYCLING HYPOXIA?

The early work of Chaplin and Durand suggested that there was a dominant cycle time of 20–30 min for fluctuations in hypoxia, based on the dye mismatch studies outlined above (23,24, 38). On the other hand, the work of Brown suggested that slower variations in  $pO_2$  may also occur, since his work involved a 24-h interval between killing hypoxic cells and irradiation (22).

In engineering studies a common way to identify cycle times in complex dynamic data sets is to use what is called Fourier transform. This mathematical operation can determine which frequencies exist in a complex time series of data. Braun *et al.* were the first to apply Fourier transform analysis to experimental measurements of laser Doppler blood flow and pO<sub>2</sub> measurements in rat muscle and tumors using microelectrodes (39). The measurements were obtained at a very high frequency (25 Hz), so this analysis could easily pick up any physiological function (such as heart rate or breathing frequency) that might influence the dynamic changes in tissue parameters. They did not observe any frequencies in the range of those associated with heart rate or breathing frequency, thus eliminating those systemic physiological factors as being involved. The dominant frequencies were <2 cycles/min and occurred in both tumor and muscle. The main difference between the two tissues was that the magnitude of fluctuations was much higher in tumor. Fourier analysis of temporally changing pO<sub>2</sub> microsensor and hemoglobin saturation data has now been performed in other tumor types (9,40-42), including spontaneous canine tumors (43). Variations in magnitude and frequency have been observed, but frequencies are well below 2 cycles/min. There have been tumor line dependent variations on the percentage of time that the pO<sub>2</sub> values reside below 10 mmHg, a convenient threshold for “hypoxia”, since most normal tissues reside at pO<sub>2</sub> values higher than that (6,42,43). Laser Doppler blood flow measurements have been performed in human tumors, and the data are consistent with what has been reported herein, but formal Fourier analysis was not performed in this case (44).

Using matched hypoxia marker drugs that were given simultaneously or separated in time by up to 96 h, Bennewith reported that the most dramatic changes in binding mismatch in the SiHa human tumor xenograft occurred in the first 12 h, followed by a more gradual increase in mismatch up to 96 h. They concluded that the predominant period for cycling hypoxia was occurring within intervals of 12 h. If one performs careful analysis of vascular networks in window chambers over time, rather dramatic changes in vascular architecture and vascular oxygen concentration can be observed to occur from day to day as part of the ongoing angiogenic process (45,46); this is consistent with the idea of cycle times on the order of several hours to days in periodicity. In one clinical report, <sup>18</sup>F misonidazole hypoxia PET imaging (47) was done on several patients with a 3-day interval between the imaging sessions (48). Hypoxic regions, as assessed by PET, changed in position, shape or size in some patients. Thus, in humans, there may be a periodicity as long as days in length, but such differences could also be explained by higher-frequency cycles as well.

We recently conducted a series of experiments in skin fold window chamber tumors, in which we measured microvessel diameter, flow rate and hemoglobin saturation every 6 h for 24 h. In these experiments, striking variations in all of these parameters were observed, yet there was a strong correlation between peak flow velocity and perfusion compared to hemoglobin saturation. These results strongly suggest that fluctuations in the delivery of oxygen contribute to cycling hypoxia on a time scale of many hours.

In summary, these reports suggest that fluctuations in tumor pO<sub>2</sub> occur in most solid tumors, but whether the fluctuations are sufficient to cause cycling hypoxia will depend upon the relative state of oxygenation and the magnitude of the fluctuations. We use the analogy of tides and waves to explain this concept more fully (Fig. 2). One might think of a small atoll in the middle of the Pacific Ocean. At high tide, the atoll may be completely covered with water, such that the waves that wash over it have no effect on how much beach is exposed. But, at low tide, the atoll is now exposed and the waves that wash on shore will cyclically cover up part of the beach and then recede. In the same way, if the overall oxygenation state of a tumor region is high, then fluctuations in the oxygen delivery may not have much of an effect on hypoxia. In contrast, in regions where the oxygenation state is marginal, fluctuations in oxygen delivery could lead to cycling hypoxia.

There is strong evidence from several different laboratories that the fastest component of cycling tumor hypoxia occurs with a frequency of a few cycles per hour. There may be a slower component that occurs over many hours to days that is related to changes in vascular network structure that occurs as a consequence of angiogenesis. Further work is required to more fully understand this slower component.

## WHAT ARE THE SPATIAL CHARACTERISTICS OF CYCLING HYPOXIA?

One of the first attempts to ascertain spatial characteristics of perfusion in tumors was performed using dynamic contrast MRI (DCE-MRI) (49). The investigators used a tissue isolated R3230Ac mammary tumor, which has a single artery and single vein. The relative simplicity permitted determination of the arterial input function, which is needed for quantitative measurements. The contrast agent used was D<sub>2</sub>O. Serial observations of the same tumor showed twofold differences in mean perfusion, as measured every 30 min for three cycles. There were spatial variations in the magnitude of change, but continuity in direction of change was observed in sets of contiguous pixels. A more recent study reported the results of serial DCE-MRI studies performed an hour apart, using a conventional gadolinium-based contrast agent (50). These studies also demonstrated quite substantial spatial and temporal variations in perfusion (Fig. 3).

Cardenas-Navia *et al.* used phosphorescence lifetime imaging of skin fold window chamber tumors to examine the spatio-temporal characteristics of cycling hypoxia in three different rat tumor lines (51). Measurements were performed every 2.5 min for 60–90 min. Fourier transform analysis of these data revealed dominant cycle times consistent with those reported for invasive probe measurements. However, there was substantial inter- and intratumoral heterogeneity in the spatial relatedness of the fluctuations. In the same tumor, some subregions would show increases in pO<sub>2</sub>, whereas other regions would be declining simultaneously. The 9L glioma exhibited very little spatial relatedness in fluctuations, whereas a mammary carcinoma and a fibrosarcoma line exhibited much greater spatial relatedness. These results suggested that the fluctuations with the fibrosarcoma line were much more tied to vascular network behavior than that seen for the 9L glioma. This was the first time that spatial statistics were used to describe the spatial relatedness of the kinetics of cycling hypoxia (Fig. 4).

Baudelet *et al.* examined the issue of spatial relatedness of pO<sub>2</sub> fluctuations using BOLD MRI (52,53). The T<sub>2</sub>\* parameter, which can be derived from the MRI signal, is sensitive to hemoglobin saturation. Deoxyhemoglobin is paramagnetic and is detectable by MRI, whereas fully oxygenated hemoglobin is diamagnetic and is not observable with MRI. The investigators measured T<sub>2</sub>\* every 25 s for periods of up to 1 h. They observed two patterns of fluctuation: one that clearly exhibited up-and-down fluctuation and one that often showed a slow decline in signal with no recovery by the end of the observation period. The pixels that exhibited up-and-down fluctuation commonly were not coordinated with adjacent pixels, whereas the regions that exhibited slow declines in T<sub>2</sub>\* were often contiguous over many pixels. By following the T<sub>2</sub>\* measurements with a terminal DCE-MRI scan, they were able to conclude that the most dynamic changes in T<sub>2</sub>\* tended to occur in highly vascular regions with relatively high permeability. This suggested that more immature vasculature might be involved in the fluctuations. In a subsequent study, the investigators reported that fluctuations were more prominent in regions that were unresponsive to the vasoconstrictive effects of CO<sub>2</sub> gas (53). This result confirms their earlier result, since immature microvessels would tend to have less smooth muscle and would therefore be less reactive to CO<sub>2</sub>.

## ARE CHRONIC AND CYCLING HYPOXIA DISTINCT PATHOPHYSIOLOGICAL ENTITIES WITHIN TUMORS, OR DO THEY EMANATE FROM THE SAME UNDERLYING PATHOLOGY?

The likelihood that a tumor region will experience cycling hypoxia is increased if the oxygen saturation of the blood entering that region is relatively low. Thus one cannot separate the fundamental factors that govern oxygen delivery (outlined above) from cycling hypoxia. There are regions of tumor that are distantly removed from microvessels, and fluctuations in red cell flux surrounding such regions may not affect the tissue oxygen concentration if it is already very low. However, we recently reported that cycling hypoxia can be observed as much as 130  $\mu\text{m}$  from a microvessel, which is near the maximum diffusion distance of oxygen (34). Complete vascular stasis is relatively uncommon and may or may not lead to complete hypoxia, depending upon the oxygenation state and density of surrounding microvessels (34). Finally, the complexity of cycling hypoxia kinetics makes it difficult to comprehend how to distinguish one entity from another. With cycle times that vary from 1–2 h to day-to-day variations, there is not a clear distinction between chronic and cycling hypoxia.

## ARE THE CONSEQUENCES OF CYCLING HYPOXIA DIFFERENT FROM THOSE ASSOCIATED WITH CHRONIC HYPOXIA?

### Phenotypic and Clinical Observations

There are several published clinical reports that tie the presence of tumor hypoxia to greater likelihood for metastasis (54,55). These will not be detailed here. Here we will focus on a comparison of what is known about the effects of chronic and cycling hypoxia on metastases. Some of the most comprehensive preclinical work on this subject has been from the laboratory of Richard Hill. This group has published several reports on the relationship between hypoxia and tumor metastasis (56-58). First, they demonstrated that the metastatic frequency of the KHT tumor was dependent upon the degree of hypoxia observed in the primary tumor when grown in the flank of recipient mice (58). Using an ingenious method to exacerbate cycling hypoxia by having mice switch breathing gas between room air and a relatively hypoxic gas several times a day, they were able to show substantial increases in metastases from the same tumor line (57). The work that they did with the ME-180 cervix cancer xenograft model is particularly interesting. Here they were able to demonstrate that cycling hypoxia increased the frequency of metastasis to regional lymph nodes after orthotopic transplantation in the cervix (56). There was also an associated increase in the expression of metastasis associated genes such as CXCR4, uPAR, VEGF and osteopontin in tumors of mice exposed to the cycling hypoxia regimen (59). In more recent studies, they have shown that cycling hypoxia increases oxidative stress in mammary tumors of the MMTV-PyMT transgenic mouse, as assessed by evidence for oxidative DNA damage (8-oxo-dG) and lipid peroxidation (60,61). In this model there was not a significant increase in metastatic frequency of mice exposed to cycling hypoxia, in spite of the evidence for increased oxidative stress (60,61).

Rofstad *et al.* used a clever combination of end points to distinguish acute from chronic hypoxia in two different melanoma xenografts *in situ* without resorting to manipulation of cycling hypoxia (62). First, they determined the fraction of radiobiologically hypoxic cells by using the *in vivo-in vitro* method referred to earlier from the work of Martin Brown (22). Since the irradiation was given in less than 5 min, this fraction would presumably represent the combination of both chronic and acutely hypoxic cells. Second, they used immunohistochemical assessment of hypoxia marker drug (pimonidazole) binding to tissue to estimate the chronically hypoxic fraction. The rationale for this came from *in vitro* experiments showing that tumor cells had to remain hypoxic for several hours to exhibit pimonidazole

binding *in vitro*. The difference between the radiobiologically hypoxic fraction and the chronic hypoxic fraction was defined to be representative of the “acute” hypoxic fraction. Using this method in primary transplanted tumors that were removed after they reached a predetermined volume, they clearly determined a positive association between the acute hypoxic fraction in the primary tumors and the incidence of pulmonary and lymph node metastases. Further, they showed that the association with metastatic frequency was significantly better using the acute hypoxic fraction as opposed to the chronic hypoxic fraction (63). These results are very intriguing, because they suggest that some tumors have more of an inherent tendency to exhibit cycling hypoxia, even when derived from the same tumor line initially. Put another way, any fluctuations in oxygenation in the small time frame over which the assay was done would not likely have been the sole cause for the increase in metastatic behavior; tumors with increased likelihood to metastasize must have had a long history of cycling hypoxia. These results suggest that diagnostic methods that could identify tumors with a tendency toward cycling hypoxia might help to identify patients who are at higher risk of metastasis.

The phenotypic differences in metastatic efficiency seen with cycling and chronic hypoxia may be caused by changes in gene expression. It is well established that cells respond to hypoxia by up-regulating a number of cellular responses; the most notable of these are the HIF-1 response, mTOR (mammalian target of rapamycin), the unfolded protein response and ATM/ATR regulation of cell cycle checkpoint control (15,64). Detailed discussions of each of these responses are provided in other reviews and will not be repeated here (6,15,64,65).

## HIF-1

HIF-1 is a transcription factor that contains two subunits, HIF-1 $\alpha$  and HIF-1 $\beta$ . Under appropriate conditions, these two proteins heterodimerize in the nucleus and bind to promoter regions of a plethora of genes involved in angiogenesis, metabolic adaptation to hypoxia, resistance to oxidative stress and increased invasive properties (65). HIF-1 $\alpha$  protein levels are tightly regulated by several mechanisms, but the most notable of these is the degradation pathway. Degradation is mediated by a family of prolyl hydroxylases that hydroxylate proline residues in the oxygen-dependent degradation (ODD) domain of HIF-1 $\alpha$  for recognition by the VHL complex that subsequently targets it for degradation via the proteasome. Under normally oxygenated conditions, HIF-1 $\alpha$  levels are reduced substantially as a result of this degradation pathway. Under hypoxic conditions, the prolyl hydroxylases cease to function properly because they require molecular oxygen for the hydroxylation. Consequently HIF-1 $\alpha$  levels increase, and it binds to HIF-1 $\beta$ . The complex enters the nucleus to bind to hypoxia responsive elements in the promoter region of many genes (65).

It has recently been shown that cells that are subjected to cycling hypoxia may exhibit a more robust HIF-1 response than cells that are chronically hypoxic. Martinive *et al.* examined the effects of cycling and chronic hypoxia on angiogenesis and tumor response to radiation therapy (66). Endothelial cells exposed to cycling hypoxia were more prone to migrate and form tubes *in vitro* as well as being more radioresistant compared with normally oxygenated or chronically hypoxic cells. This effect appeared to be mediated by HIF-1 $\alpha$ , because knockdown of HIF-1 by siRNA abrogated the radioresistance. Tumors grown in mice that were subjected to cycles of hypoxic air breathing were more radioresistant than mice that breathed room air. Irradiation was given during air breathing in both cases. Peng *et al.* examined the carotid body response of wild-type and HIF-1 $\alpha$  haploinsufficient mice to periods of cycling hypoxia in simulation of sleep apnea (repeated cycles of 15 s hypoxia at 10% O<sub>2</sub> followed by 5 min of air breathing) (67). Here they found that the physiological responses of wild-type mice were more striking than the heterozygous mice and that the responses appeared to be mediated by elevated levels of reactive oxygen species in the wild-type mice. Ning *et al.* recently reported that mild periods of cycling hypoxia resulted in a more robust HIF-1 response than more severe hypoxia in an



isolated perfused heart model (68). Collectively, these results suggest that cycling hypoxia may exert a more profound influence on HIF-1 levels and transcriptional activity, but additional research on this subject is clearly warranted.

## mTOR

mTOR is a component of the mTORC complex, which functions in cells primarily to sense changes in nutrients, energy status or oxidative stress. It is a serine/threonine protein kinase that regulates cell proliferation, motility and survival by regulating, among other things, protein synthesis and gene transcription (69,70). It appears that HIF-1 and mTOR are involved in a feedback loop that is mediated by hypoxia. Hypoxia is known to down-regulate mTOR activity via an indirect mechanism through the HIF-1-regulated proteins Redd1, Redd 2 and Bnip3 (70). Alternatively, Hudson reported that inhibition of mTOR using rapamycin led to increased HIF-1 degradation in the presence of the hypoxia mimic CoCl<sub>2</sub> and speculated that mTOR regulates HIF-1 primarily by influencing its rate of degradation (71). However, Yuan *et al.* recently reported that cycling hypoxia up-regulates mTOR-regulated synthesis of HIF-1 $\alpha$  protein, which leads to increased transcriptional activity (72). Thus it appears that the interaction between HIF-1 and mTOR is very dependent on context and that cycling hypoxia may influence mTOR activity in a manner that is diametrically opposed to that of chronic hypoxia.

## Unfolded Protein Response (UPR)

The unfolded protein response relates to changes in cell function that occur when cells are stressed (64,73). The consequences of activation of the UPR include changes in protein production and maturation, cell metabolic response and death (64). Most notably, hypoxia and oxidative stress are strong inducers of the UPR (64). One of the hallmarks of the stress response is the formation of stress granules, which are complexes formed from small ribosomal subunits, mRNA and protein, which restrict access of mRNAs to the endoplasmic reticulum and down-regulate protein synthesis (74). We were among the first to show that stress granules form during hypoxia both *in vitro* and *in vivo* and that reoxygenation that occurs after radiation therapy leads to disaggregation of these granules and restoration of protein synthesis (75) (Fig. 5). HIF-1-regulated genes are among the types that are retained in stress granules, and once they disaggregate, they are rapidly translated into protein. It takes a few hours for the stress granules to form and/or disaggregate; thus one might expect that stress granule formation and disaggregation might occur in response to cycling hypoxia, particularly since there is evidence for an increase in oxidative stress as a consequence of cycling hypoxia in tumors (61).

## IS THERE EVIDENCE FOR CYCLING HYPOXIA IN HUMAN AND CANINE TUMORS?

There are only a handful of papers published on this subject. Pigott *et al.* examined blood flow in a series of superficial human tumors, using implanted laser Doppler flow probes, for periods of 1 h (44). In about 50% of the lesions studied, they observed fluctuations in red cell flux of a factor of >1.5, with kinetics similar to what has been reported for mouse models for this time frame. Since red cell flux variations appear to be most closely tied to cycling hypoxia in murine models (33,34), one could surmise that this is indirect evidence for cycling hypoxia. However, they did not know what the overall oxygenation state of the tissue was in these tumors, so it is difficult to know for certain whether these fluctuations were commensurate with hypoxia reoxygenation. In a small series of canine tumors, pO<sub>2</sub> fluctuations were also measured using invasive probes (43). In this series, fluctuations were observed and cycles of oxygenation sufficient to cause hypoxia reoxygenation were observed. There was no correlation between the overall oxygenation state of the tumors and the incidence of cycling hypoxia.

Janssen *et al.* used an immunohistochemical method to detect evidence for cycling hypoxia in 46 patients with head and neck cancer (76). These patients had been administered the thymidine analogue IdUrd prior to biopsy. Integration of this analogue into the DNA of cycling cells can be detected by immunohistochemistry. Tumor sections were stained for vessels and the presence of perivascular IdUrd uptake. Vessels that did not exhibit perivascular IdUrd staining were presumed to be exhibiting acute hypoxia. The frequency of mismatch ranged from 1–40%. The assumption underlying complete mismatch is that acute hypoxia is a result of total vascular stasis, which as explained above, is not necessary for cycling hypoxia to occur. Nevertheless, these data probably represent a conservative estimate of the fraction of tumor that might be experiencing cycling hypoxia at any given time.

$^{18}\text{F}$  misonidazole PET has also been used to assess the frequency of cycling hypoxia in head and neck cancer (77). Misonidazole is a bioreductive drug that is selectively retained in hypoxic cells. When labeled with  $^{18}\text{F}$ , it can be detected using PET. In this small series of seven patients, two PET scans were performed 3 days apart prior to the onset of therapy. In four of seven patients, either the hypoxic subvolume changed substantially in volume or the shape or distribution of hypoxic subvolumes changed. These data represent the only direct validation that cycling hypoxia may exist in human tumors. Clearly one has to be cautious in not overinterpreting such a result, and much more work is required to verify such a result with larger numbers of patients and in more than one tumor site (Fig. 6). The clinical relevance for this observation is important in the context of intensity-modulated radiotherapy. For example, a therapeutic strategy that targets the placement of higher radiation doses to the hypoxic subvolume would be difficult to accomplish if the subvolume moves from day to day or even hour to hour unless there were a method to identify it on the treatment couch at the time of each radiation fraction. Such methods do not currently exist.

## SUMMARY

In this review, I have summarized the historical findings of pioneers in the field of radiobiology who first discovered the phenomenon of cycling hypoxia, using radiation as a tool to uncover it. The pathological physiological features of cycling hypoxia and discussed the potential implications of instability of oxygenation on gene expression and cellular function were summarized. It is clear that the kinetics of cycling hypoxia is complex and that further work is needed to characterize it more firmly. Finally, I have provided a glimpse of human data, suggesting that this phenomenon does occur in patients. Clearly, there is much more work to do. We need to determine whether this feature of hypoxia carries independent predictive power for treatment outcome, compared with more traditional methods for assessing hypoxia, such as implantable oxygen sensors, immunohistochemistry or imaging methods. We need to better understand the implications of cycling hypoxia on gene expression and cell function to decipher whether there are new therapeutic targets created by cycling hypoxia. Finally, we need to establish means to better study it in human subjects.

## Acknowledgments

This work was supported by a grant from the NIH/NCI CA0355. The author wishes to thank the following individuals, in no particular order, who contributed substantially to the thinking encompassed in this review: Brian Sorg, Benjamin Moeller, Yiting Cao, Thies Schroeder, Isabel Cardenas-Navia, Rod Braun, Jennifer Lanzen, David Brizel and Chuan Li. The author thanks Ashley Manzoor for helping to create Fig. 2 and Eui Jung Moon for administrative support.

## REFERENCES

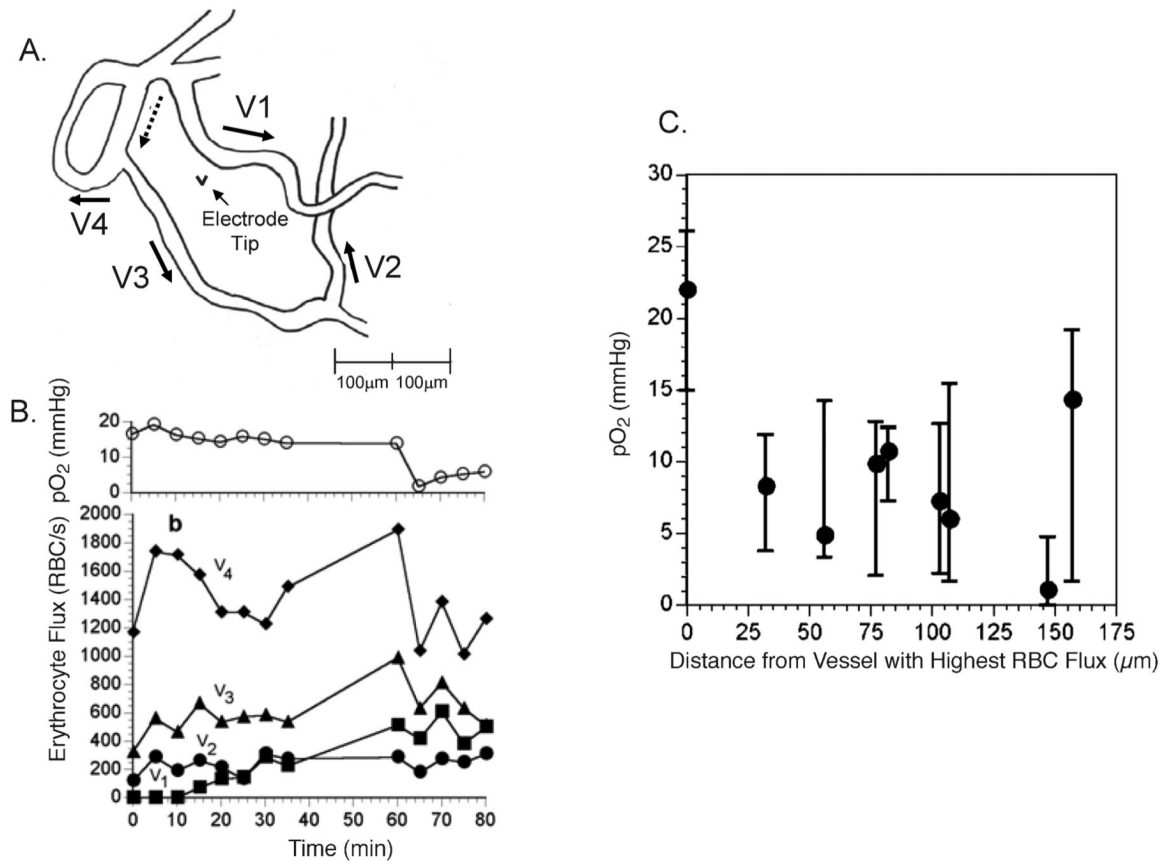
1. Semenza GL, Wang GL. A nuclear factor induced by hypoxia via de novo protein synthesis binds to the human erythropoietin gene enhancer at a site required for transcriptional activation. *Mol. Cell. Biol.* 1992;12:5447–5454. [PubMed: 1448077]

2. Wang GL, Semenza GL. General involvement of hypoxia-inducible factor 1 in transcriptional response to hypoxia. *Proc. Natl. Acad. Sci. USA* 1993;90:4304–4308. [PubMed: 8387214]
3. Risau W. Mechanisms of angiogenesis. *Nature* 1997;386:671–674. [PubMed: 9109485]
4. Ferrara N, Davis-Smyth T. The biology of vascular endothelial growth factor. *Endocr. Rev* 1997;18:4–25. [PubMed: 9034784]
5. Neufeld G, Cohen T, Gengrinovitch S, Poltorak Z. Vascular endothelial growth factor (VEGF) and its receptors. *FASEB J* 1999;13:9–22. [PubMed: 9872925]
6. Dewhirst MW, Cao Y, Moeller B. Cycling hypoxia and free radicals regulate angiogenesis and radiotherapy response. *Nat. Rev* 2008;8:425–437.
7. Dewhirst MW, Ong ET, Braun RD, Smith B, Klitzman B, Evans SM, Wilson D. Quantification of longitudinal tissue pO<sub>2</sub> gradients in window chamber tumours: impact on tumour hypoxia. *Br. J. Cancer* 1999;79:1717–1722. [PubMed: 10206282]
8. Dewhirst MW, Ong ET, Klitzman B, Secomb TW, Vinuya RZ, Dodge R, Brizel D, Gross JF. Perivascular oxygen tensions in a transplantable mammary tumor growing in a dorsal flap window chamber. *Radiat. Res* 1992;130:171–182. [PubMed: 1574573]
9. Sorg BS, Hardee ME, Agarwal N, Moeller BJ, Dewhirst MW. Spectral imaging facilitates visualization and measurements of unstable and abnormal microvascular oxygen transport in tumors. *J. Biomed. Opt* 2008;13:014026. [PubMed: 18315384]
10. Secomb TW, Hsu R, Dewhirst MW, Klitzman B, Gross JF. Analysis of oxygen transport to tumor tissue by microvascular networks. *Int. J. Radiat. Oncol. Biol. Phys* 1993;25:481–489. [PubMed: 8436527]
11. Dewhirst MW, Kimura H, Rehmus SW, Braun RD, Papahadjopoulos D, Hong K, Secomb TW. Microvascular studies on the origins of perfusion-limited hypoxia. *Br. J. Cancer* 1996;27:S247–251.
12. Kavanagh BD, Coffey BE, Needham D, Hochmuth RM, Dewhirst MW. The effect of flunarizine on erythrocyte suspension viscosity under conditions of extreme hypoxia, low pH, and lactate treatment. *Br. J. Cancer* 1993;67:734–741. [PubMed: 8471430]
13. Eddy HA, Casarett GW. Development of the vascular system in the hamster malignant neurilemmoma. *Microvasc. Res* 1973;6:63–82. [PubMed: 4125277]
14. Secomb TW, Hsu R, Ong ET, Gross JF, Dewhirst MW. Analysis of the effects of oxygen supply and demand on hypoxic fraction in tumors. *Acta Oncol* 1995;34:313–316. [PubMed: 7779415]
15. Bristow RG, Hill RP. Hypoxia and metabolism. Hypoxia, DNA repair and genetic instability. *Nat. Rev* 2008;8:180–192.
16. Sanderson JC. A new method for the microscopic study of living growing tissues in the rabbit's ear. *Anat. Rec* 1924;28:281–287.
17. Goodall CM, Sanders AG, Shubik P. Studies of vascular patterns in living tumors with a transparent chamber inserted in hamster cheek pouch. *J. Natl. Cancer Inst* 1965;35:497–521. [PubMed: 5835038]
18. Algire GH. An adaptation of the transparent-chamber technique to the mouse. *J. Natl. Cancer Inst* 1943;4:1–11.
19. Asaishi K, Endrich B, Gotz A, Messmer K. Quantitative analysis of microvascular structure and function in the amelanotic melanoma A-Mel-3. *Cancer Res* 1981;41:1898–1904. [PubMed: 7214358]
20. Yamaura H, Matsuzawa T. Tumor regrowth after irradiation; an experimental approach. *Int. J. Radiat. Biol. Relat. Stud. Phys. Chem. Med* 1979;35:201–219. [PubMed: 222702]
21. Rockwell S, Kallman RF. Cellular radiosensitivity and tumor radiation response in the EMT6 tumor cell system. *Radiat. Res* 1973;53:281–294. [PubMed: 4695229]
22. Brown JM. Evidence for acutely hypoxic cells in mouse tumours, and a possible mechanism of reoxygenation. *Br. J. Radiol* 1979;52:650–656. [PubMed: 486895]
23. Chaplin DJ, Durand RE, Olive PL. Acute hypoxia in tumors: implications for modifiers of radiation effects. *Int. J. Radiat. Oncol. Biol. Phys* 1986;12:1279–1282. [PubMed: 3759546]
24. Trotter MJ, Chaplin DJ, Durand RE, Olive PL. The use of fluorescent probes to identify regions of transient perfusion in murine tumors. *Int. J. Radiat. Oncol. Biol. Phys* 1989;16:931–934. [PubMed: 2703399]
25. Durand RE, Aquino-Parsons C. Non-constant tumour blood flow—implications for therapy. *Acta Oncol* 2001;40:862–869. [PubMed: 11859987]

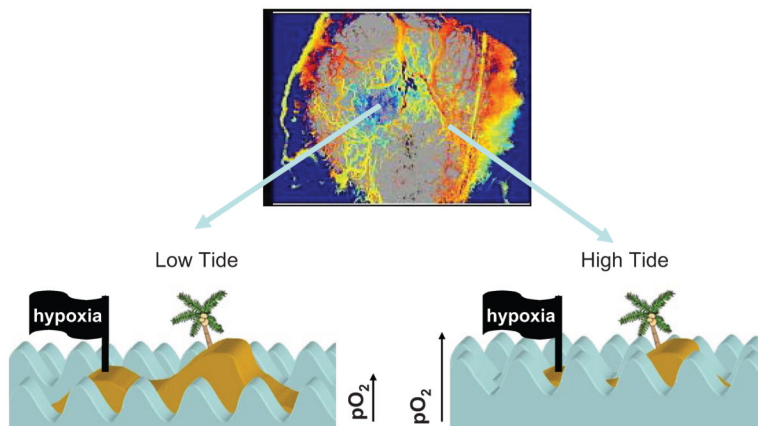
26. Bennewith KL, Durand RE. Quantifying transient hypoxia in human tumor xenografts by flow cytometry. *Cancer Res* 2004;64:6183–6189. [PubMed: 15342403]
27. Bennewith KL, Raleigh JA, Durand RE. Orally administered pimonidazole to label hypoxic tumor cells. *Cancer Res* 2002;62:6827–6830. [PubMed: 12460894]
28. Koch CJ. Measurement of absolute oxygen levels in cells and tissues using oxygen sensors and 2-nitroimidazole EF5. *Methods Enzymol* 2002;352:3–31. [PubMed: 12125356]
29. Raleigh JA, Dewhirst MW, Thrall DE. Measuring tumor hypoxia. *Semin. Radiat. Oncol* 1996;6:37–45. [PubMed: 10717160]
30. Helmlinger G, Yuan F, Dellian M, Jain RK. Interstitial pH and pO<sub>2</sub> gradients in solid tumors *in vivo*: high-resolution measurements reveal a lack of correlation. *Nat. Med* 1997;3:177–182. [PubMed: 9018236]
31. Rumsey WL, Vanderkooi JM, Wilson DF. Imaging of phosphorescence: a novel method for measuring oxygen distribution in perfused tissue. *Science* 1988;241:1649–1651. [PubMed: 3420417]
32. Skala MC, Fontanella A, Hendargo H, Dewhirst MW, Izatt JA. Combined hyperspectral and spectral domain optical coherence tomography microscope for non-invasive hemodynamic imaging. *Optics Lett* 2009;34:289–291.
33. Kimura H, Braun RD, Ong ET, Hsu R, Secomb TW, Papahadjopoulos D, Hong K, Dewhirst MW. Fluctuations in red cell flux in tumor microvessels can lead to transient hypoxia and reoxygenation in tumor parenchyma. *Cancer Res* 1996;56:5522–5528. [PubMed: 8968110]
34. Lanzen J, Braun RD, Klitzman B, Brizel D, Secomb TW, Dewhirst MW. Direct demonstration of instabilities in oxygen concentrations within the extravascular compartment of an experimental tumor. *Cancer Res* 2006;66:2219–2223. [PubMed: 16489024]
35. Kiani MF, Pries AR, Hsu LL, Sarelius IH, Cokelet GR. Fluctuations in microvascular blood flow parameters caused by hemodynamic mechanisms. *Am. J. Physiol* 1994;266:H1822–H1828. [PubMed: 8203581]
36. Zakrzewicz A, Secomb TW, Pries AR. Angioadaptation: keeping the vascular system in shape. *News Physiol. Sci* 2002;17:197–201. [PubMed: 12270956]
37. Patan S, Munn LL, Jain RK. Intussusceptive microvascular growth in a human colon adenocarcinoma xenograft: a novel mechanism of tumor angiogenesis. *Microvasc Res* 1996;51:260–272. [PubMed: 8778579]
38. Chaplin DJ, Olive PL, Durand RE. Intermittent blood flow in a murine tumor: radiobiological effects. *Cancer Res* 1987;47:597–601. [PubMed: 3791244]
39. Braun RD, Lanzen JL, Dewhirst MW. Fourier analysis of fluctuations of oxygen tension and blood flow in R3230Ac tumors and muscle in rats. *Am. J. Physiol* 1999;277:H551–H568. [PubMed: 10444480]
40. Brurberg KG, Graff BA, Olsen DR, Rofstad EK. Tumor-line specific pO<sub>2</sub> fluctuations in human melanoma xenografts. *Int. J. Radiat. Oncol. Biol. Phys* 2004;58:403–409. [PubMed: 14751509]
41. Brurberg KG, Graff BA, Rofstad EK. Temporal heterogeneity in oxygen tension in human melanoma xenografts. *Br. J. Cancer* 2003;89:350–356. [PubMed: 12865929]
42. Cardenas-Navia LI, Yu D, Braun RD, Brizel DM, Secomb TW, Dewhirst MW. Tumor-dependent kinetics of partial pressure of oxygen fluctuations during air and oxygen breathing. *Cancer Res* 2004;64:6010–6017. [PubMed: 15342381]
43. Brurberg KG, Skogmo HK, Graff BA, Olsen DR, Rofstad EK. Fluctuations in pO<sub>2</sub> in poorly and well-oxygenated spontaneous canine tumors before and during fractionated radiation therapy. *Radiother. Oncol* 2005;77:220–226. [PubMed: 16257074]
44. Pigott KH, Hill SA, Chaplin DJ, Saunders MI. Microregional fluctuations in perfusion within human tumours detected using laser Doppler flowmetry. *Radiother. Oncol* 1996;40:45–50. [PubMed: 8844886]
45. Cao Y, Li CY, Moeller BJ, Yu D, Zhao Y, Dreher MR, Shan S, Dewhirst MW. Observation of incipient tumor angiogenesis that is independent of hypoxia and hypoxia inducible factor-1 activation. *Cancer Res* 2005;65:5498–5505. [PubMed: 15994919]
46. Dewhirst MW, Cao Y, Li CY, Moeller B. Exploring the role of HIF-1 in early angiogenesis and response to radiotherapy. *Radiother. Oncol* 2007;83:249–255. [PubMed: 17560674]

47. Ljungkvist AS, Bussink J, Kaanders JH, van der Kogel AJ. Dynamics of tumor hypoxia measured with bioreductive hypoxic cell markers. *Radiat. Res* 2007;167:127–145. [PubMed: 17390721]
48. Nehmeh SA, Lee NY, Schroder H, Squire O, Zanzonico PB, Erdi YE, Greco C, Mageras G, Pham HS, Humm JL. Reproducibility of intratumor distribution of <sup>18</sup>F-fluoromisonidazole in head and neck cancer. *Int. J. Radiat. Oncol. Biol. Phys* 2008;70:235–242. [PubMed: 18086391]
49. Eskey CJ, Koretsky AP, Domach MM, Jain RK. <sup>2</sup>H-nuclear magnetic resonance imaging of tumor blood flow: spatial and temporal heterogeneity in a tissue-isolated mammary adenocarcinoma. *Cancer Res* 1992;52:6010–6019. [PubMed: 1394226]
50. Brurberg KG, Benjaminsen IC, Dorum LM, Rofstad EK. Fluctuations in tumor blood perfusion assessed by dynamic contrast-enhanced MRI. *Magn. Reson. Med* 2007;58:473–481. [PubMed: 17763357]
51. Cardenas-Navia LI, Mace D, Richardson RA, Wilson DF, Shan S, Dewhirst MW. The pervasive presence of fluctuating oxygenation in tumors. *Cancer Res* 2008;68:5812–5819. [PubMed: 18632635]
52. Baudelet C, Ansiaux R, Jordan BF, Havaux X, Macq B, Gallez B. Physiological noise in murine solid tumours using T2\*-weighted gradient-echo imaging: a marker of tumour acute hypoxia? *Phys. Med. Biol* 2004;49:3389–3411. [PubMed: 15379021]
53. Baudelet C, Cron GO, Ansiaux R, Crockart N, DeWever J, Feron O, Gallez B. The role of vessel maturation and vessel functionality in spontaneous fluctuations of T2\*-weighted GRE signal within tumors. *NMR Biomed* 2006;19:69–76. [PubMed: 16411170]
54. Vaupel P, Hockel M, Mayer A. Detection and characterization of tumor hypoxia using pO<sub>2</sub> histography. *Antioxid. Redox Signal* 2007;9:1221–1235. [PubMed: 17536958]
55. Moon EJ, Brizel DM, Chi JT, Dewhirst MW. The potential role of intrinsic hypoxia markers as prognostic variables in cancer. *Antioxid. Redox Signal* 2007;9:1237–1294. [PubMed: 17571959]
56. Cairns RA, Hill RP. Acute hypoxia enhances spontaneous lymph node metastasis in an orthotopic murine model of human cervical carcinoma. *Cancer Res* 2004;64:2054–2061. [PubMed: 15026343]
57. Cairns RA, Kalliomaki T, Hill RP. Acute (cyclic) hypoxia enhances spontaneous metastasis of KHT murine tumors. *Cancer Res* 2001;61:8903–8908. [PubMed: 11751415]
58. De Jaeger K, Kavanagh MC, Hill RP. Relationship of hypoxia to metastatic ability in rodent tumours. *Br. J. Cancer* 2001;84:1280–1285. [PubMed: 11336482]
59. Chaudary N, Hill RP. Increased expression of metastasis-related genes in hypoxic cells sorted from cervical and lymph nodal xenograft tumors. *Lab. Invest* 2009;89:587–596. [PubMed: 19308047]
60. Kalliomaki TM, McCallum G, Wells PG, Hill RP. Progression and metastasis in a transgenic mouse breast cancer model: effects of exposure to *in vivo* hypoxia. *Cancer Lett* 2009;282:98–108. [PubMed: 19356843]
61. Kalliomaki TM, McCallum G, Lunt SJ, Wells PG, Hill RP. Analysis of the effects of exposure to acute hypoxia on oxidative lesions and tumour progression in a transgenic mouse breast cancer model. *BMC Cancer* 2008;8:151. [PubMed: 18507854]
62. Rofstad EK, Maseide K. Radiobiological and immunohistochemical assessment of hypoxia in human melanoma xenografts: acute and chronic hypoxia in individual tumours. *Int. J. Radiat. Biol* 1999;75:1377–1393. [PubMed: 10597912]
63. Rofstad EK, Galappathi K, Mathiesen B, Ruud EB. Fluctuating and diffusion-limited hypoxia in hypoxia-induced metastasis. *Clin. Cancer Res* 2007;13:1971–1978. [PubMed: 17360973]
64. Wouters BG, Koritzinsky M. Hypoxia signalling through mTOR and the unfolded protein response in cancer. *Nat. Rev* 2008;8:851–864.
65. Semenza GL. Targeting HIF-1 for cancer therapy. *Nat. Rev* 2003;3:721–732.
66. Martinive P, Defresne F, Bouzin C, Saliez J, Lair F, Gregoire V, Michiels C, Dessy C, Feron O. Preconditioning of the tumor vasculature and tumor cells by intermittent hypoxia: implications for anticancer therapies. *Cancer Res* 2006;66:11736–11744. [PubMed: 17178869]
67. Peng YJ, Yuan G, Ramakrishnan D, Sharma SD, Bosch-Marce M, Kumar GK, Semenza GL, Prabhakar NR. Heterozygous HIF-1alpha deficiency impairs carotid body-mediated systemic responses and reactive oxygen species generation in mice exposed to intermittent hypoxia. *J. Physiol* 2006;577:705–716. [PubMed: 16973705]

68. Ning XH, Chen SH, Buroker NE, Xu CS, Li FR, Li SP, Song DS, Ge M, Hyyti OM, Portman MA. Short-cycle hypoxia in the intact heart: hypoxia-inducible factor 1alpha signaling and the relationship to injury threshold. *Am. J. Physiol* 2007;292:H333–H341.
69. Hay N, Sonenberg N. Upstream and downstream of mTOR. *Genes Dev* 2004;18:1926–1945. [PubMed: 15314020]
70. Dunlop EA, Tee AR. Mammalian target of rapamycin complex 1: Signalling inputs, substrates and feedback mechanisms. *Cell. Signal* 2009;21:827–835. [PubMed: 19166929]
71. Hudson CC, Liu M, Chiang GG, Otterness DM, Loomis DC, Kaper F, Giaccia AJ, Abraham RT. Regulation of hypoxia-inducible factor 1alpha expression and function by the mammalian target of rapamycin. *Mol. Cell. Biol* 2002;22:7004–7014. [PubMed: 12242281]
72. Yuan G, Nanduri J, Khan S, Semenza GL, Prabhakar NR. Induction of HIF-1alpha expression by intermittent hypoxia: involvement of NADPH oxidase, Ca<sup>2+</sup> signaling, prolyl hydroxylases, and mTOR. *J. Cell. Physiol* 2008;217:674–685. [PubMed: 18651560]
73. Dang Y, Kedersha N, Low WK, Romo D, Gorospe M, Kaufman R, Anderson P, Liu JO. Eukaryotic initiation factor 2alpha-independent pathway of stress granule induction by the natural product pateamine A. *J. Biol. Chem* 2006;281:32870–32878. [PubMed: 16951406]
74. Arimoto K, Fukuda H, Imajoh-Ohmi S, Saito H, Takekawa M. Formation of stress granules inhibits apoptosis by suppressing stress-responsive MAPK pathways. *Nat. Cell Biol* 2008;10:1324–1332. [PubMed: 18836437]
75. Moeller BJ, Cao Y, Li CY, Dewhirst MW. Radiation activates HIF-1 to regulate vascular radiosensitivity in tumors: role of reoxygenation, free radicals, and stress granules. *Cancer Cell* 2004;5:429–441. [PubMed: 15144951]
76. Janssen HL, Ljungkvist AS, Rijken PF, Sprong D, Bussink J, van der Kogel AJ, Haustermans KM, Begg AC. Thymidine analogues to assess microperfusion in human tumors. *Int. J. Radiat. Oncol. Biol. Phys* 2005;62:1169–1175. [PubMed: 15990022]
77. Lin Z, Mechalakos J, Nehmeh S, Schoder H, Lee N, Humm J, Ling CC. The influence of changes in tumor hypoxia on dose-painting treatment plans based on <sup>18</sup>F-FMISO positron emission tomography. *Int. J. Radiat. Oncol. Biol. Phys* 2008;70:1219–1228. [PubMed: 18313529]
78. Kety S. Theory of blood-tissue exchange and its application to measurements of blood flow. *Methods Med. Res* 1960;8:228–236.

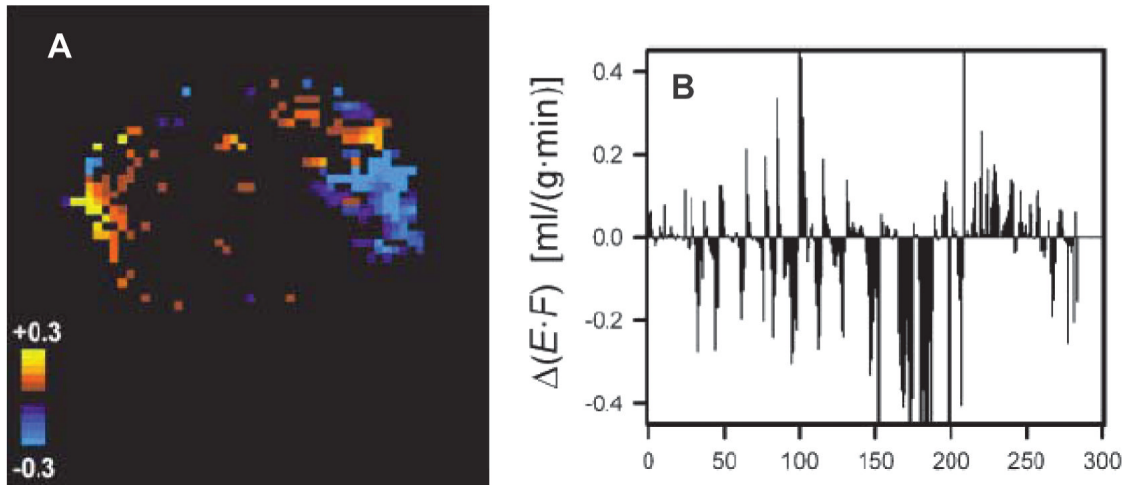
**FIG. 1.**

Relationship between red cell flux variation and interstitial pO<sub>2</sub> in a skin fold window chamber tumor. Panel A: Tracing of vascular field, taken from a video monitor, indicating direction of flow for segments surrounding an interstitial location for pO<sub>2</sub> measurement. Panel B: Time tracings of red cell flux and interstitial pO<sub>2</sub> for an 80-min observation period. Note that the interstitial pO<sub>2</sub> drops toward the end of the period, commensurate with a reduction in red cell flux. Panel C: Summary figure from several experiments showing the median and magnitude of fluctuations in pO<sub>2</sub> as a function of distance from the microvessel in each preparation with the highest red cell flux. These data strongly suggest that cycling hypoxia can exist near the diffusion limit of oxygen. Oxygen tension measurements were made using recessed tip oxygen microelectrodes with tip diameters <10 μm. Figure adapted from Lanzen *et al.* with permission from the author and publisher (34).

**FIG. 2.**

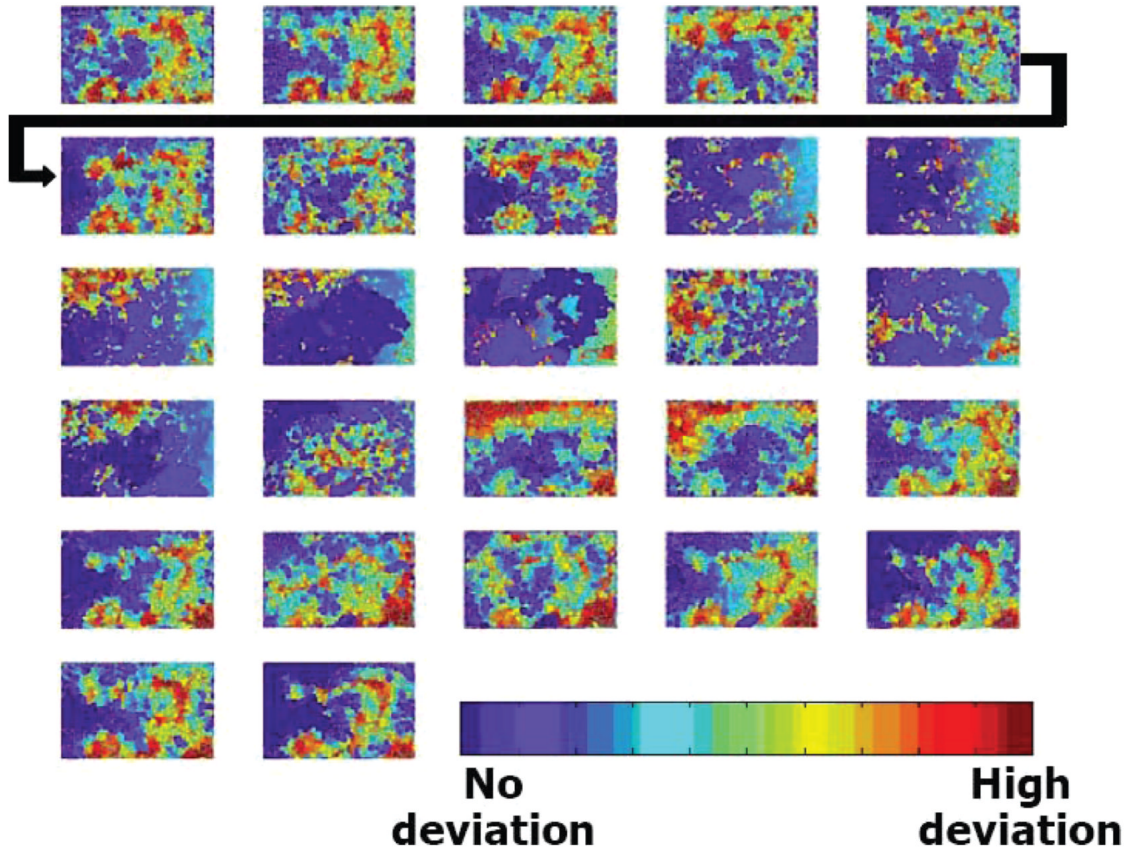
Analogy between tides and waves and cycling hypoxia. Oxygen transport in tumors is somewhat analogous to the effect of high and low tides on how far waves crash on to the beach of an island. If the tide is low, then the waves do not travel very far up the beach, but when tide is high, the waves can travel much farther. In an analogous fashion, some networks of tumor vessels can have relatively little oxygen available (low tide), whereas in the same tumor, other networks may have an overabundance of oxygen (high tide). In both cases, though, the amount of oxygen delivered is unstable over time (analogous to the waves), and the tumor cells (analogous to the beach) experience the same instability. The upper panel shows a map of hemoglobin saturation ( $Hb_{sat}$ ) in a window chamber tumor. The central portion (blue) shows blood vessels with low  $Hb_{sat}$ , indicating that they are not carrying very much oxygen (they were perfused, however, based on visual inspection). The peripheral portion of the tumor exhibits microvessels with much higher  $Hb_{sat}$ . The lower panel depicts the analogy with the island, showing the net effect of the tides and waves on water coverage over the beach. In the case of cycling hypoxia in tumors, however, the kinetics of oxygen instability is quite complex (not like regular waves), with high (<1 cycle/h), intermediate (<24 h) and slow (>24-h cycle times). In addition, there are circumstances where  $pO_2$  drops to a very low level for long periods (severe chronic hypoxia), which would be insufficient to support cell survival.



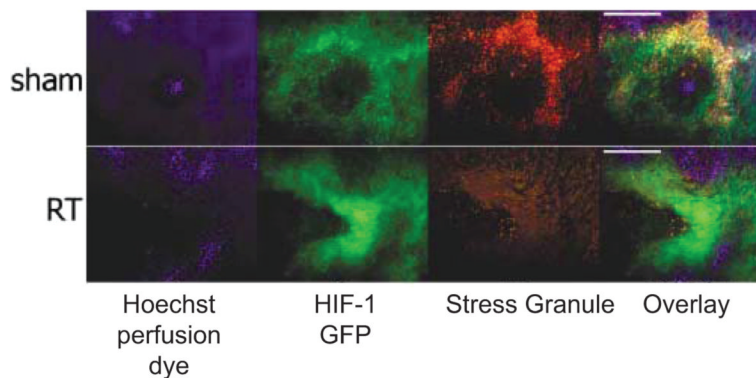


**FIG. 3.**

Changes in perfusion within an A-07 melanoma xenograft, as assessed by two DCE-MRI studies done 1 h apart. The parameter  $E \cdot F$  is derived from the Kety equation (78) and is an estimate of perfusion.  $\Delta E \cdot F$  is the difference between the two studies. Panel A: The color code indicates a change in perfusion of more than 0.03 ml/(g·min), which was considered significant. Note that in the same tumor, there are regions that increase (yellow) and decrease (blue) between the two studies. Panel B:  $\Delta E \cdot F$  is plotted as a function of pixel number (arbitrary assignment). Corroborating panel A, there are significant increases and decreases in  $\Delta E \cdot F$  within the same tumor. The connection between contiguous pixels, with respect to direction of change, suggests that changes in vascular network perfusion patterns are responsible for this effect. DCE-MRI refers to dynamic contrast enhanced MRI. This is a method to assess the dynamic changes in MRI contrast as a function of time after injection in a tissue of interest. Figure adapted from Brurberg *et al.* with permission from the author and publisher (50).



**FIG. 4.** Spatial relatedness of cycling hypoxia obtained using phosphorescence lifetime imaging of a skin fold window chamber containing the R3230Ac mammary carcinoma. Watershed segmentation results are shown for 2.5-min intervals. Time increased from left to right, top to bottom, in 2.5-min increments. Watershed segmentation creates boundaries at sharp gradients in pO<sub>2</sub>; segmented regions can be thought of as pO<sub>2</sub> isobars. Segments are color-coded by their deviations from the median pO<sub>2</sub> of the image. Red, high deviations from the median; blue, no deviation from the median. Figure adapted from Cardenas Navia *et al.* with permission from the author and publisher (51).

**FIG. 5.**

Changes in stress granule prominence in response to reoxygenation after radiation therapy (RT) in the 4T1 mouse mammary tumor. Hoechst 33342, a perfusion marker dye, was administered to mice intravenously a few minutes prior to tumor removal. Perfused vessels will show perivascular Hoechst 33342 staining of tumor cell nuclei (blue). HIF-1-GFP is a reporter gene for HIF-1 expression (green). Stress granules were identified using an antibody to one of the constituent proteins that form the granules (red). The upper row shows a sham-irradiated tumor. Hoechst 33342 shows the heaviest uptake in regions of low HIF-1 GFP expression. Stress granules are in high density in regions of HIF-1 GFP expression (yellow shows overlap). The lower row shows a tumor treated with  $3 \times 5$  Gy and removed 24 h after last radiation dose. GFP expression is higher than the control, but there is a reduction in the density of stress granules and overlap with HIF-1 GFP. In data not shown, the tumors exhibited strong reoxygenation during this period, even though HIF-1 GFP expression was elevated. Thus a reduction in stress granule density was associated with a period of reoxygenation after radiotherapy. It is likely that stress granule formation and disaggregation occurs during cycling hypoxia. Bar = 50  $\mu$ m. Figure adapted from Moeller *et al.* with permission of the author and publisher (75).

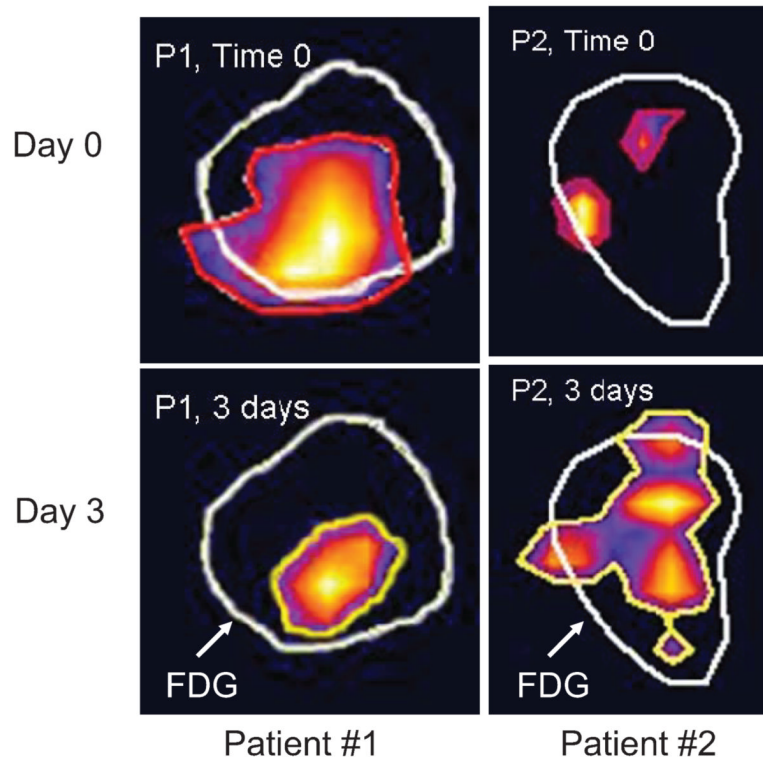


**FIG. 6.** Differences in  $^{18}\text{F}$  misonidazole uptake as assessed by PET scans taken 3 days apart in patients with head and neck cancer. In these scans, the  $^{18}\text{F}$  FDG (fluorodeoxyglucose) avid area is outlined in white and the areas positive for  $^{18}\text{F}$  misonidazole are outlined in red (time 0) and yellow (time 3 days). In patient 1, the region of hypoxia remains in the same location but shrinks between day 0 and day 3. In patient 2, the regions of hypoxia change in size and distribution between the 2 days. This is the first evidence for cycling hypoxia in human subjects. Data courtesy of Clif Ling, John Humm and Nancy Lee. Related data can be found in Lin *et al.* (77).